Near-field imaging and frequency tuning of a high-Q photonic crystal membrane microcavity

S. Mujumdar[1,2], A. F. Koenderink[1,3], T. Sünner[4], B. C. Buchler[1,5], M. Kamp[4], A. Forchel[4], and V. Sandoghdar[1*]

[1]*Laboratory of Physical Chemistry and optETH, ETH Zurich, CH-8093 Zurich, Switzerland*

[2]*Current address: Tata Institute of Fundamental Research, Homi Bhabha Road, Mumbai, 400 005, India*

[3]*Current address: Center for Nanophotonics, FOM Institute AMOLF, Kruislaan 407, NL-1098SJ Amsterdam, The Netherlands*

[4]*Technische Physik, Universität Würzburg, Am Hubland, D-97074 Würzburg, Germany*

[5]*Current address: ARC Centre of Excellence for Quantum Atom Optics, Department of Physics, The Australian National University, Canberra, Australia*

[*]*Corresponding author: vahid.sandoghdar@ethz.ch*

Abstract: We discuss experimental studies of the interaction between a nanoscopic object and a photonic crystal membrane resonator of quality factor Q=55000. By controlled actuation of a glass fiber tip in the near field of the photonic crystal, we constructed a complete spatio-spectral map of the resonator mode and its coupling with the fiber tip. On the one hand, our findings demonstrate that scanning probes can profoundly influence the optical characteristics and the near-field images of photonic devices. On the other hand, we show that the introduction of a nanoscopic object provides a low loss method for on-command tuning of a photonic crystal resonator frequency. Our results are in a very good agreement with the predictions of a combined numerical/analytical theory.

OCIS codes: (180.4243) Near-field microscopy; (230.5298) Photonic crystals; (130.4815) Optical switching devices; (270.0270) Quantum optics

References and links

1. D. W. Pohl, W. Denk, and M. Lanz, "Optical stethoscopy: Image recording with resolution lambda/20," Appl. Phys. Lett. **44,** 651-653 (1984).
2. A. Lewis, M. Isaacson, A. Harootunian, and A. Murray, "Experimental strategy in three-dimensional structure determination of crotoxin complex thin crystal," Ultramicroscopy **13**, 27-34, (1984).
3. V. Sandoghdar, "Trends and developments in scanning near-field optical microscopy," pp. 65-119, *Nanometer Scale Science and Technology*, (IOS Press, Amsterdam, 2001).
4. W. P. Ambrose, P. M. Goodwin, J. C. Martin, and R. A. Keller, "Alterations of Single Molecule Fluorescence Lifetimes in Near-Field Optical Microscopy," Science **265**, 364-367 (1994).
5. H. Gersen, M. F. Garcia-Parajo, L. Novotny, J. A. Veerman, L. Kuipers, and N. F. van Hulst, "Influencing the Angular Emission of a Single Molecule," Phys. Rev. Lett. **85**, 5312-5315 (2000).
6. I. Gerhardt, G. Wrigge, M. Agio, P. Bushev, G. Zumofen, and V. Sandoghdar, "Scanning near-field optical coherent spectroscopy of single molecules at 1.4K," Opt. Lett. **32**, 1420-1422 (2007).

#88320 - $15.00 USD Received 8 Oct 2007; revised 17 Nov 2007; accepted 17 Nov 2007; published 10 Dec 2007

7. K. Vahala, "Optical Microcavities," Nature **424**, 839 (2003).
8. O. Painter, R. K. Lee, A. Scherer, A. Yariv, J. D. O'Brien, P. D. Dapkus, and I. Kim, "Two-Dimensional Photonic Band-Gap Defect Mode Laser," Science **284**, 1819-1821 (1999).
9. B.-S. Song, S. Noda, T. Asano, and Y. Akahane, "Ultra-high-Q photonic double-heterostructure nanocavity," Nat. Mater. **4**, 207-210 (2005).
10. R. Herrmann, T. Suenner, T. Hein, A. Löffler, M. Kamp, and A. Forchel, "Ultrahigh-quality photonic crystal cavity in GaAs," Opt. Lett. **31**, 1229-1231 (2006).
11. T. Tanabe, M. Notomi, E. Kuramochi, A. Shinya, and H. Taniyama, "Trapping and delaying photons for one nanosecond in an ultrasmall high-Q photonic-crystal nanocavity," Nat. Photonics **1**, 49-52 (2007).
12. C. M. Soukoulis, ed., *Photonic band gap materials*, (Kluwer, Dordrecht, 1996).
13. J. D. Joannopoulos, R. D. Meade, and J. N. Winn, *Photonic Crystals* (Princeton University Press, Princeton, N.J., 1995).
14. V. Sandoghdar, B. C. Buchler, P. Kramper, S. Götzinger, O. Benson, and M. Kafesaki, "Scanning near-field optical studies of photonic devices," *Photonic Crystals* (Wiley-VCH, Weinheim, Germany, 2004).
15. M. L. M. Balistreri, H. Gersen, J. P. Korterik, L. Kuipers, and N. F. van Hulst, "Tracking Femtosecond Laser Pulses in Space and Time," Science **294**, 1080-1082 (2000).
16. S. I. Bozhevolnyi, V. S. Volkov, J. Arentoft, A. Boltasseva, T. Søndergaard, and M. Kristensen, "Direct mapping of light propagation in photonic crystal waveguides," Opt. Commun. **212**, 51-55 (2002).
17. P. Kramper, M. Kafesaki, C. M. Soukoulis, A. Birner, F. Müller, U. Gösele, R. B. Wehrspohn, J. Mlynek, and V. Sandoghdar, "Near-field visualization of light confinement in a photonic crystal microresonator," Opt. Lett. **29**, 174-176 (2004).
18. K. Srinivasan, P. E. Barclay, M. Borselli, and O. Painter, " Optical-fiber-based measurement of an ultrasmall volume high-Q photonic crystal microcavity," Phys. Rev. B **70**, 081306R (2004).
19. R. Wüest, B.C. Buchler, D. Erni, R. Harbers, P. Strasser, A. F. Koenderink, F. Robin, V. Sandoghdar, and and H. Jäckel, "A standing-wave meter to measure dispersion and loss of photonic-crystal waveguides," Appl. Phys. Lett. **87**, 261110 (2005).
20. N. Louvion, A. Rahmani, C. Seassal, S. Callard, D. Gerard, and F. de Fornel, "Near-field observation of sub-wavelength confinement of photoluminescence by a photonic crystal microcavity," Opt. Lett. **31**, 2160-2162, (2006).
21. A. F. Koenderink, M. Kafesaki, B. C.Buchler, and V. Sandoghdar, " Controlling the Resonance of a Photonic Crystal Microcavity by a Near-Field Probe," Phys. Rev. Lett. **95**, 153904 (2005).
22. I. Märki, M. Salt, and H.-P. Herzig, "Tuning the resonance of a photonic crystal microcavity with an AFM probe," Opt. Express **14**, 2969-2978 (2006).
23. W. C. L. Hopman, K. O. van der Werf, A. J. F. Hollink, W. Bogaerts, V. Subramaniam, and R. M. de Ridder, "Nano-mechanical tuning and imaging of a photonic crystal micro-cavity resonance," Opt. Express **14**, 8745-8752 (2006).
24. L. Lalouat, B. Cluzel, P. Velha, E. Picard, D. Peyrade, J. P. Hugonin, P. Lalanne, E. Hadji, and F. de Fornel, "Near-field interactions between a subwavelength tip and a small-volume photonic-crystal nanocavity," Phys. Rev. B **76**, 041102(R) (2007).
25. Y. Akahane, T. Asano, B. S. Song, and S. Noda, "High-Q photonic nanocavity in a two-dimensional photonic crystal," Nature **425**, 944 (2003).
26. K. Srinivasan, P. E. Barclay, O. Painter, J. Chen, A. Y. Cho, and C. Gmachl, "Experimental demonstration of a high quality factor photonic crystal microcavity," Appl. Phys. Lett. **83**, 1915-1917 (2003).
27. E. Weidner, S. Combrié, N. Tran, A. DeRossi, J. Nagle, S. Cassette, A. Talneau, and H. Benisty, "Achievement of ultrahigh quality factors in GaAs photonic crystal membrane nanocavity," Appl. Phys. Lett. **89**, 221104 (2006).
28. T. Skauli, P. S. Kuo, K. L. Vodopyanov, T. J. Pinguet, O. Levi, L. A. Eyres, J. S. Harris, M. M. Fejer, B. Gerard, L. Becouarn and E. Lallier, "Improved dispersion relations for GaAs and applications to nonlinear optics," J. Appl. Phys. **94**, 6447-6455 (2003).
29. A. Taflove and S. C.Hagness, *Computational Electrodynamics: the Finite-Difference Time-Domain Method. – 3rd ed.* (Artech House, Norwood, MA, 2005).
30. S. Fan, I. Appelbaum, and J. D. Joannopoulos, "Near-field scanning optical microscopy as a simultaneous probe of fields and band structure of photonic crystals: A computational study," Appl. Phys. Lett. **75**, 3461-3463 (1999).
31. O. Hess, C. Hermann, and A. Klaedtke, "Finite-Difference Time-Domain simulations of photonic crystal defect structures," Phys. Status Solidi A **197**, 605-619 (2003).
32. M. Loncar, A. Scherer, and Y. Qiu, "Photonic crystal laser sources for chemical detection," Appl. Phys. Lett. **82**, 4648-4650 (2003).
33. M. Barth and O. Benson, "Manipulation of dielectric particles using photonic crystal cavities," Appl. Phys. Lett. **89**, 253114 (2006).

Scanning near-field optical microscopy (SNOM) [1, 2] is in principle capable of offering an infinitely high optical resolution. This technique examines the nonpropagating evanescent op-

#88320 - $15.00 USD Received 8 Oct 2007; revised 17 Nov 2007; accepted 17 Nov 2007; published 10 Dec 2007

tical fields by scanning a subwavelength probe [3]. In the vast majority of the applications, it has been assumed that the probe does not perturb the information obtained from the sample under study. However, a few reports have shown that the fluorescence properties of dye molecules could be modified by the SNOM tip [4, 5, 6]. In this article, we experimentally show and theoretically analyze the influence of a SNOM tip on the spatial and spectral distributions of light in a high-Q photonic crystal resonator. Our results have important implications for SNOM imaging, controlled tuning of high-Q photonic devices and optical sensing.

Microcavities have stimulated a great deal of activity in design and fabrication of new optical systems [7]. For most applications in quantum optics, integrated optics and optical sensing it is desirable to increase Q and decrease the mode volume V. As the microcavities become smaller though, the Q often begins to degrade either because of the relative importance of surfaces or because of diffraction losses. Resonators based on photonic crystal (PC) structures offer a good compromise [8, 9, 10, 11]. By controlling the subwavelength features of PC structures, scientists have demonstrated their potential for molding the flow of light [12, 13]. However, the intrinsic sensitivity of a PC performance to its nanoscopic features also imposes stringent demands on its fabrication accuracy. Considering that today's control in nanofabrication is still not sufficient to produce PCs with the exact design parameters, it is imperative to 1) characterize the end product and 2) fine tune its properties after manufacturing. In this work, we address both of these issues in the near field.

In the past few years, several groups have demonstrated the power of SNOM and related techniques for imaging light propagation and confinement in PC structures [14, 15, 16, 17, 18, 19, 20]. Recently, we theoretically analyzed the influence of a nano-object on the spectral resonance and the intensity distribution of a PC microresonator with $Q = 13000$. We concluded that depending on the polarizability of the tip, its influence might no longer be negligible for cavities of low V and high Q [21]. We found that in general, the tip could introduce a frequency shift and a broadening in the resonance of the PC mode. However, we also showed that the effect of the tip could be exploited to one's advantage for tuning the microcavity resonance by a large amount *without* inflicting a significant broadening [21]. Indeed, the promise of this technique has been already recognized and the first experimental attempts along this line have been pursued by applying silicon tips to PC cavities with low Qs of the order of 500 [22, 23]. The observed frequency shifts in these efforts were accompanied by substantial broadenings of the cavity resonances. In another study, a metallic tip was used to tune the resonance of a one-dimensional PC cavity with Q of the order of 1000 [24]. Demonstration of resonance tuning on high-Q PC cavities has not been reported.

The design of high-Q PC resonators has witnessed a tremendous progress in the last five years [25, 26]. Nevertheless, structures with $Q \gg 10000$ have been available only from a handful of groups because in addition to a suitable design, they have to meet stringent fabrication requirements [9, 27, 10, 11]. Devices based on silicon have reached extremely high Q values beyond 10^6 [11], but GaAs based structures have been more difficult to master [27, 10]. As depicted in Fig. 1(a), we have used a line-defect heterostructure cavity design [9] realized by connecting crystals with lattice parameters $a_1 = 410$ nm, $a_2 = 400$ nm and $r/a = 0.23$ in a 221 nm thick GaAs membrane ($\varepsilon = 11.39$) [28]. A collinear W1 waveguide throughout the two lattices resulted in a mode gap in the transmission band diagram of the structure, confining light in the longitudinal direction, while the photonic bandgap confined light in the transverse direction. Two heterostructures were further created on either side of the cavity to facilitate incoupling and outcoupling of light. The details of the fabrication procedure are reported in Ref. [10].

Linearly polarized laser light from a grating-tunable diode laser (linewidth < 300 KHz, tuning range 1550 nm - 1630 nm) was focussed onto one end facet of the membrane using a large

#88320 - $15.00 USD Received 8 Oct 2007; revised 17 Nov 2007; accepted 17 Nov 2007; published 10 Dec 2007

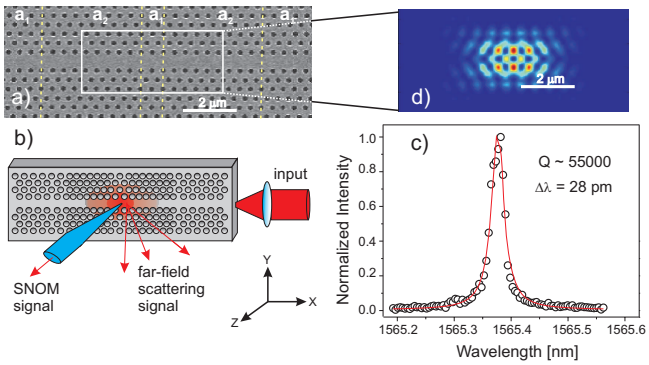

Fig. 1. Scanning electron micrograph of the heterostructure. The yellow lines mark regions with different lattice constants. a_1=410 nm, a_2 = 400 nm. (b) Schematics of the experimental arrangement. (c) The unperturbed cavity resonance as measured in the far field. The red curve is a Lorentzian fit to the measured data (black circles). (d) The calculated (FDTD) intensity distribution on resonance in the region marked by the white rectangle in Fig. (a).

numerical aperture lens (NA = 0.68). To facilitate the incoupling, the W1 waveguide of the cavity was gradually enlarged to a W3 waveguide at the input facet of the fabricated membrane. As sketched in Fig. 1(b), a small fraction of light is typically scattered from the surface of a PC resonator. This light was detected using a lens system and was sent to a sensitive InGaAs camera or avalanche photodiode (APD) to perform spectroscopy on the passive resonator. Figure 1(c) displays an experimental spectrum centered at λ =1565.38 and a Lorentzian fit, yielding a linewidth of 28 pm corresponding to $Q = 55000$. We point out that over the months that our measurements were made, the Q remained the same, but the cavity resonance frequency shifted by up to 0.6 nm. We attribute this to environmental changes such as temperature variations or deposition of tiny amount of adsorbates. As a result, the exact resonance frequencies discussed in what follows might differ from one study to the next although they were all performed on the same PC resonator. Figure 1(d) shows the light intensity distribution within the cavity on resonance calculated using the three-dimensional finite difference time domain (FDTD) method [29, 30]. We employed Liao absorbing boundary conditions with grid spacings $a/14$ in the lateral and $a/28$ in the vertical dimensions and used volume averaging of epsilon to improve the resolution [31].

As depicted in Fig. 1(b), we employed a SNOM setup to access the cavity mode in the near field. We used a sharp uncoated heat-pulled fiber tip (diameter $\sim$ 100 nm) glued onto a quartz tuning fork. Shear-force tip-sample distance stabilization was used to maintain the tip at a distance of about 10 nm from the membrane and to image the sample topography. The optical fiber tip detected the evanescent light intensity above the surface using the InGaAs APD at a typical resolution of 100 nm. Figure 2 shows tiles of recorded images illustrating the near-field intensity distribution recorded at various fixed wavelengths close to the cavity resonance. At $\lambda = 1565.1$ nm (tile A), one can see the light propagating from the left through the W1 waveguide. At $\lambda = 1565.16$ nm, the light intensity begins to enter the cavity region, but it also leaks into the PC structure (tiles B & C). At $\lambda = 1565.2$ nm (tile D), most of the intensity is concentrated into a bright elliptical locus just outside the waveguide. Upon traversing this highest intensity point, the pattern becomes sharper and gradually collapses into itself until it ends at a bright point in the center of the cavity (tiles E-K, $\lambda = 1565.22$ nm-1565.5 nm). Beyond this point the waveguide mode dominates again (tiles L & M). Note that the intensity in each image has been normalized separately so the waveguide light is overwhelmed in images D-

#88320 - $15.00 USD Received 8 Oct 2007; revised 17 Nov 2007; accepted 17 Nov 2007; published 10 Dec 2007

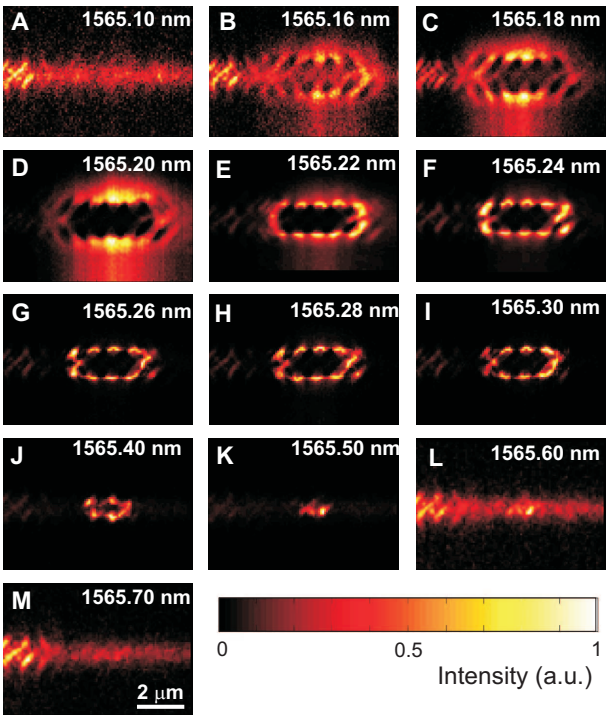

Fig. 2. Tiles A through M represent SNOM images of the intensity distribution in the PC structure at different wavelengths indicated in each image. Each image is normalized independently according to the color scale shown.

K. These measurements show the first near-field measurements of light distribution in a high-Q PC cavity. They also reveal a drastic *spatial* variation of the intensity distribution within a very narrow wavelength range. We emphasize that if the tip were simply imaging the unperturbed cavity intensity distribution, we would expect that all the images D-K should resemble Fig. 1(d). Instead we see dramatic changes of the intensity pattern suggesting that, at a given wavelength, the cavity will resonate only for a specific locus of tip positions.

In order to verify our experimental findings and their interpretation, one could perform computationally intensive FDTD calculations for each tip position. However, a faster and more instructive check could be achieved by applying the perturbative treatment described in Ref. [21]. The frequency detuning $\Delta\omega$ induced by the tip, or in general a nanoscopic perturber, is given by,

$$\frac{\Delta\omega}{\omega} = -\frac{\alpha_{eff}}{2}\frac{|E_0(\mathbf{r}_\parallel)|^2}{\int \varepsilon(\mathbf{r})|E_0|^2 d\mathbf{r}}\exp(-z_p/d) \quad (1)$$

where $\alpha_{eff} = 3V_{eff}(\varepsilon_p - 1)/(\varepsilon_p + 2)$ is the perturber's effective polarizability, z_p is its separation from the sample, and d is the interaction length of the evanescent part of the cavity mode, found to be 50 nm in FDTD calculations [21]. We used the results of the 3D FDTD calculations for $|E_0|^2$ shown in Fig. 1(d), the typical value of $r_p = 50$ nm for an uncoated SNOM tip, and the perturber effective volume $V_{eff} = \pi r_p^2 d$ to compute the resonance frequency detuning $\Delta\omega$ at each pixel. Next, we took into account a Lorentzian profile with a full width at half-maximum of 28 pm (see Fig. 1(c)) for the cavity spectrum and then calculated the intensity of light at a wavelength of interest. A selection of the results corresponding to or very close

#88320 - $15.00 USD Received 8 Oct 2007; revised 17 Nov 2007; accepted 17 Nov 2007; published 10 Dec 2007

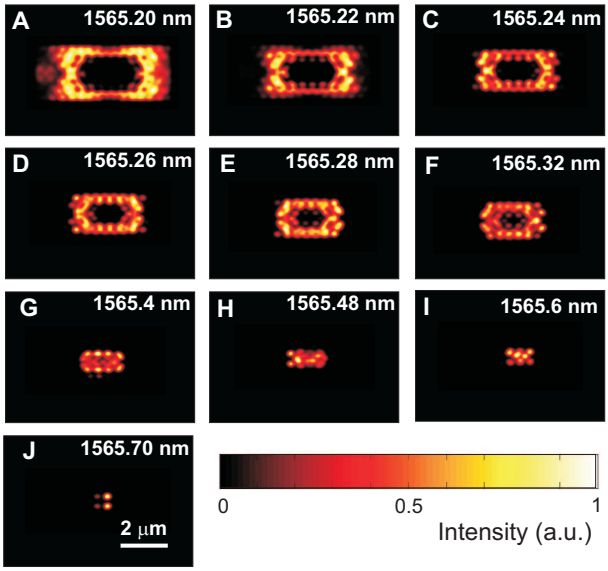

Fig. 3. Calculated intensity distribution at different wavelengths, based on 3D FDTD simulations supplemented with first-order perturbation calculations to take into account the impact of the fiber tip. At each wavelength, the structure is resonant with the incident laser for selected locations of the tip. The calculation only considered the cavity mode without the waveguide mode. Each image is normalized independently according to the color scale shown.

to the wavelengths of the experimental images in Fig. 2D-M are presented in Fig. 3A-J. We remark that since the FDTD calculations did not consider the waveguide mode, the theoretical images in Fig. 3 do not reproduce Figs. 2A-C or Figs. 2L-M. In fact, Figs. 3I-J indicate that the experimental images of Figs. 2L-M are dominated by the waveguide mode. The theoretical and experimental results show a very good semi-quantitative agreement and confirm that the tip influences the cavity resonance frequency in a subwavelength position dependent manner.

Next, we analyzed the complete perturbation landscape by recording SNOM spectra for tip positions in the x-y plane. At each tip position, the laser wavelength was scanned, giving results such as those shown in Fig. 4(b). The wavelength of peak intensity for each tip position is plotted in Fig 4(a) to give a detailed map of the change in cavity frequency induced by the tip. Over subwavelength displacements (e.g. see the points 'A' to 'D'), the resonance shifts by more than 3 linewidths. As predicted in Ref. [21], the spatial variation of the tip-induced resonance frequency shift resembles the distribution of the intensity in the unperturbed cavity shown in Fig. 1(d). Figure 4(b) plots examples of spectra recorded at points A-D, revealing that the resonance lines could deviate from a Lorentzian shape, making it difficult to assess a quantitative measure of the *Q* degradation. However, the data clearly show that the tip-induced broadening is much smaller than the frequency shift.

In conclusion, we have used a scanning near-field probe to study the spatio-spectral features of light in a photonic crystal membrane cavity of Q=55000. The data in Figs. 1, 2, and 3 show that at any given laser frequency, the resonator admits light only if the probe is positioned with subwavelength accuracy on a specific locus of points. We expect similar results also for other cavities with high-*Q*s and small volumes. The extreme spectral and spatial sensitivities of such structures to the presence of a subwavelength object such as a tip means that SNOM images of photonic structures would have to be interpreted with care. On the other hand, these sensi-

#88320 - $15.00 USD Received 8 Oct 2007; revised 17 Nov 2007; accepted 17 Nov 2007; published 10 Dec 2007

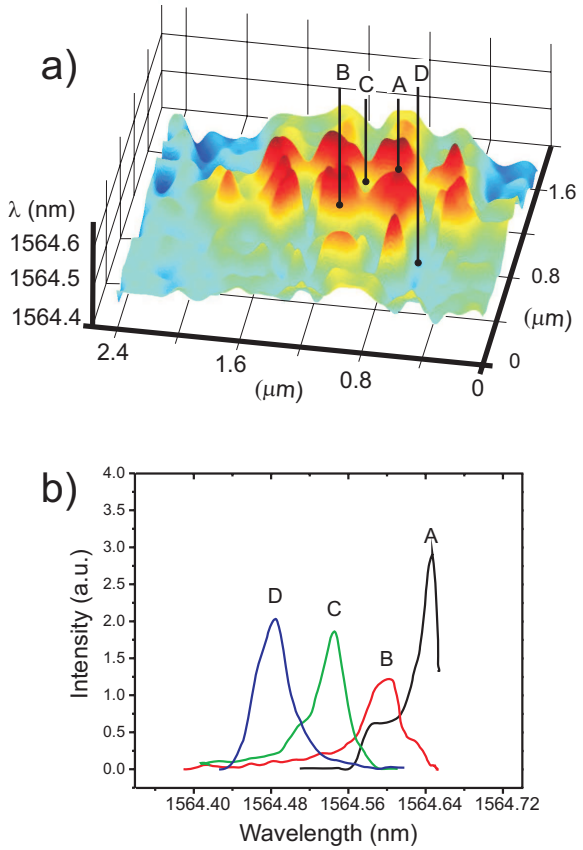

Fig. 4. a) The peak wavelengths of the detuned cavity resonance as a function of tip location. b) Four examples of the local resonance spectra measured through the SNOM tip at the indicated locations A-D in part (a).

tivities offer opportunities for a number of applications. In particular, we have demonstrated that the resonance spectrum of a microcavity can be manipulated dynamically by actuating a nanoscopic object without a notable sacrifice in the resonator *Q*. Such a nanomechanical actuation could be exploited in compact devices such as high-*Q* filters or routers. Furthermore, our findings indicate that a nanoparticle or a nanoscopic flow of fluid would result in the spectral modification of the cavity and could be used for sensing [32, 33]. High-*Q* structures are advantageous for these applications because a nano-object can change the cavity resonance frequency substantially even if it is located at fairly large distances of several tens of nanometers.

We are grateful to C. M. Soukoulis, M. Kafesaki and M. Agio for help in the early stages of our FDTD work. We are grateful to M. Quack and G. Seyfang for providing us with the laser source. We acknowledge the generous support from the Deutsche Forschungsgemeinschaft (Schwerpunktsprogramm SP1113), ETH Zurich and the European Network of Excellence ePIXnet.

#88320 - $15.00 USD Received 8 Oct 2007; revised 17 Nov 2007; accepted 17 Nov 2007; published 10 Dec 2007